Global Journal of Researches in Engineering
Mechanical and Mechanics Engineering
Volume 12 Issue 5 Version 1.0 Year 2012
Type: Double Blind Peer Reviewed International Research Journal
Publisher: Global Journals Inc. (USA)
Online ISSN: 2249-4596 Print ISSN:0975-5861

A Computational Approach on the position of Load Centre of a Slipper Bearing

By Mr Kishan Choudhuri & Dr Prasun Chakraborti
National Institute of Technology, Agartala.

Abstract - The slipper bearing is an integrated part of an axial piston pump. Proper lubrication is important for successful operation of the slipper bearing. This type of bearing is a type of hydrostatic thrust bearing. Many works have been done in the recent past on this type of bearing. This current work is based on the theoretical investigation of the locus of the load centre of this type of bearing. The leakage losses and the slipper drag are two important factors on which this type of bearing is designed. The load carrying capacity has a direct impact on those two factors. On the other hand the stability of the bearing depends upon the position of the load centre. There are many input factors on which the position of load centre is varied. These input factors thus play an important role on the smooth operation of such bearing. Such input variable are slipper tilt, applied pressure on the slipper, slipper speed, slipper non flatness angle or slipper land size. On the variation of these input variables, the nature of the position of load centre is plotted in this work. Based on the results the reasonable conclusions are made.

Index Terms : Slipper, position of load centre, slipper tilt, lubrication.

GJRE-A Classification : FOR Code: 090607

A COMPUTATIONAL APPROACHON THEPOSITION OFLOAD CENTRE OFASLIPPER BEARING

Strictly as per the compliance and regulations of:

A Computational Approach on the position of Load Centre of a Slipper Bearing

Mr Kishan Choudhuri [α] & Dr Prasun Chakraborti [σ]

Abstract - The slipper bearing is an integrated part of an axial piston pump. Proper lubrication is important for successful operation of the slipper bearing. This type of bearing is a type of hydrostatic thrust bearing. Many works have been done in the recent past on this type of bearing. This current work is based on the theoretical investigation of the locus of the load centre of this type of bearing. The leakage losses and the slipper drag are two important factors on which this type of bearing is designed. The load carrying capacity has a direct impact on those two factors. On the other hand the stability of the bearing depends upon the position of the load centre. There are many input factors on which the position of load centre is varied. These input factors thus play an important role on the smooth operation of such bearing. Such input variable are slipper tilt, applied pressure on the slipper, slipper speed, slipper non flatness angle or slipper land size. On the variation of these input variables, the nature of the position of load centre is plotted in this work. Based on the results the reasonable conclusions are made.

Index Terms : Slipper, position of load centre, slipper tilt, lubrication.

I. Introduction

Axial piston swash-plate type hydrostatic pumps are being used extensively in aircraft, industrial and agricultural systems since they can transmit large specific power and the flow rate from them can be varied. A basic difference in the design of various models of axial piston pumps is how the pistons contact the swash plate. Many design use a bronze slipper positioned between the piston and the swash plate. With this design, hydraulic fluid is fed through internal passages to the piston/slipper and slipper/swash plate interfaces to supply lubrication at these surfaces. Some axial do not use a slipper, but rather finish each piston with a case-hardened spherical dome. The spherical dome contacts the swash plate in such a fashion, much like the contact that occurs in ball bearings. Elimination of the slipper reduces costs and eliminates the disadvantages of the slipper design, but unfortunately, it creates other problems. One of these is wear at the spherical dome/swash plate interface. The fig. 1 shows a typical slipper-piston assembly. The slipper is pivoted on the ball at the end of the piston to allow it to adjust to the swash plate angle and to rotate relative to the piston. High pressure fluid from the piston is connected via the control orifices in the piston and slipper to the central slipper pool allowing covered the influence of the orifice size on the performance of the bearing. Koc and Hooke [1] examined the effect of the tilting couples on the behavior of the slippers experimentally. Wang and Yamaguchi [2], [3] clarified experimentally and theoretically the effects of nozzle and thermoplastic materials on the characteristics of hydrostatic bearing/seal parts in water hydraulic axial pumps and motors. Manring [4] investigated the effects of pressure-induced deformations on the characteristics of hydrostatic thrust bearing. Manring [5] investigated experimentally, the effect of different socket geometry in the performance of slipper bearing. They found the effect on the leakage flow, load carrying capacity and the film thickness of the slipper bearing. In the work of Nie S. L. [6], the characteristic equation of the hydrostatic slipper bearing with an annular orifice damper is formulated, where the effects of various geometric parameters (e.g. damping length, supporting length, and clearance between the piston and the cylinder bore) are reflected. S. Kumar, J.M. Bergada, J. Watton [7] presented static and dynamic characteristics of a piston pump slipper with a groove. Three dimensional Navier Stokes equations in cylindrical coordinates have been applied to the slipper/plate gap, including the groove. In the work of M. Borghi, E. Specchia and B. Zardin [8] a numerical procedure is used to solve the Reynolds equation, written here with respect to the slipper-swash plate gap, whose height is considered variable in a two dimensional field and with time. In the work of Hong Liu, Zeng Xiong Peng, Chu Jing Shen [9] the calculation of film shape is simplified as a single objective optimization problem with two decision variables. A genetic algorithm is used to investigate about the film shape of the entire slipper bearing In the work of Fazil Canbulut, Erdem Koç, Cem Sinanoglu [10], the slipper geometry and working conditions affected on the slipper performance have been analyzed experimentally. The model of the slipper system has been established by original neural network (NN) method. The objective of the present work is theoretical investigation of the position of the load centre of the slipper bearing which is not studied extensively by the previous authors.

Author α : Assistant Professor, Production Engineering Department, National Institute of Technology, Agartala, Tripura, India.
Author σ : National Institute of Technology, Agartala.

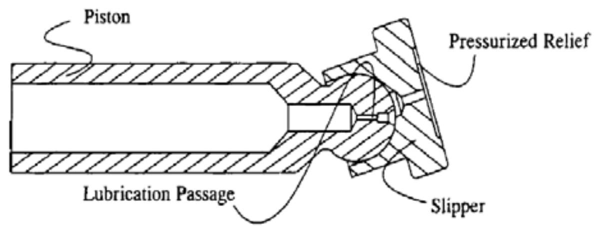

Figure 1 : Piston-slipper assembly

List of Symbols

a	Conical angle of the slipper.
$\bar{a}$	Non-dimensional value of a
a^*	Another non-dimensional form of a
d	A dimension for a conical slipper
$\bar{d}$	Non-dimensional value of d
e	A measure of slipper tilt
G	Non dimensional hydrodynamic parameter.
h	A variable defining film thickness
h_a	Average film thickness.
$\bar{h}$	Non-dimensional value of h
$\bar{h}_c$	The non dimensional film thickness at the mid radius of the land
$\bar{h}_o$	Non dimensional film thickness at middle land for no tilt
O	Orifice size coefficient
O_f	Orifice coefficient of the orifice between piston cylinder and slipper pocket.
p	Variable defining pressure in the slipper land
p_s	Pressure in slipper pocket
$\bar{p}_s$	Non-dimensional value of p_s
$\bar{p}$	Non-dimensional value of p
Q	Drain flow through the conical and tilted slipper
$\bar{Q}$	Non dimensional form of Q
r	Radius of any point on the slipper land measured from slipper center.
$\bar{r}$	Non-dimensional value of r
r_c	Mid-land radius
$\bar{r}_c$	Non dimensional mid land radius
r_i	Inner radius of slipper
$\bar{r}_i$	Non-dimensional value of r_i
r_o	Outer radius of slipper.
$\bar{r}_o$	Non-dimensional value of r_o
t	Slipper tilt in radian
$\bar{t}$	Non-dimensional value of t
t^*	Another non-dimensional form of t
u	Slipper velocity
W	Load carrying capacity for the slipper
$\bar{W}$	Non-dimensional value of W
$\bar{w}$	Non dimensional width of the slipper land
θ	Angle measured from trailing edge of the slipper
θ_d	Angle measured from the position of maximum clearance
θ_m	Angle of maximum clearance.

II. Mathematical Model

The following assumptions are taken into account to derive all the equations:

- Body forces acting on the lubricant such as gravitational, magnetic or electrical are neglected
- The pressure induced flow in the circumferential direction is neglected
- The pressure is assumed to constant through the thickness of the lubricating fluid.
- The lubricant is Newtonian.
- Viscosity is considered to be constant through the thickness of the lubricating film.
- The flow is laminar.
- Surface velocities are considered to be constant in direction.
- The lands is approximately conical.

Slipper is having a circular pocket, which is surrounded by a land as shown in figure. 1. The orifice connects the slipper pocket to the piston bore which feeds it with oil thus establishing a pressure in the slipper pocket which is approximately equal to piston pressure. The oil inside the slipper pocket lubricates the total slipper area. Referring to the Figure 2 the clearance between the land of an untilted slipper and the swash plate can be expressed as

$h = h_a - d + az + tr$. When slipper is tilted (Figure.3) this clearance becomes $h = h_a - d + az + tr\cos(\theta_d)$

And in non-dimensional form $\bar{h} = 1 - \bar{d} + \bar{a}\bar{z} + \bar{t}\bar{r}\cos(\theta_d)$

Pressure distribution over a slipper land must satisfy Reynold's equation, which is expressed in polar coordinate by:

Global Journal of Researches in Engineering (A) Volume XII Issue V Version I Year 2012

$$\frac{1}{r}\frac{\partial}{\partial r}\frac{rh^3}{12\mu}\frac{\partial p}{\partial r}+\frac{1}{r^2}\frac{\partial}{\partial\theta}\frac{h^3}{12\mu}\frac{\partial p}{\partial\theta}=$$

$$\frac{u}{2}\left[\frac{\partial h}{\partial r}\cos\theta-\frac{1}{r}\frac{\partial h}{\partial\theta}\sin\theta\right]$$

Making Non-dimensional form and introducing the non-dimensional group

$$G=\frac{\mu u r_o}{h_a^2 p_p}$$

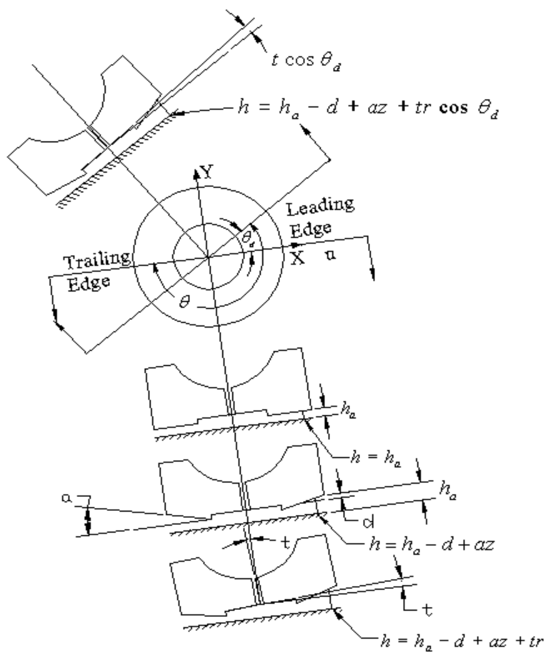

Figure 2 : The geometry of slipper bearing

$$\bar{p}=A+\frac{6G}{\bar{r}_c\bar{h}_c^3}$$

$$\left\{C\bar{z}+\left[\bar{r}_c\left(\bar{a}\cos\theta+\bar{t}\cos\theta_m\right)-\frac{C}{\bar{r}_c}-\frac{3C}{\bar{h}_c}\left(\bar{a}+\bar{t}\cos\theta_d\right)\right]\frac{\bar{z}^2}{2}\right\}$$

where $\bar{h}_c=1-\bar{d}+\bar{t}\bar{r}_c\cos\theta_d$ is the non-dimensional film thickness at the mid radius of the land. Constants A and C can be found out from the boundary conditions. The boundary conditions are

At $r=r_i$, $p=p_s$ and at $r=r_o$, $p=0$

This leads to a pressure distribution:

$$\bar{p}=\bar{p}_s\left[\frac{1}{2}-\frac{\bar{z}}{\bar{w}}+\frac{\left(\bar{z}^2-\bar{w}^2/4\right)}{2\bar{w}\bar{r}_c}\right]+\frac{3\bar{p}_s}{2\bar{w}\bar{h}_c}\left(\bar{a}+\bar{t}\cos\theta_d\right)\left(\bar{z}^2-\bar{w}^2/4\right)$$

$$+\frac{3G}{\bar{h}_c^3}\left(\bar{a}\cos\theta+\bar{t}\cos\theta_m\right)\left(\bar{z}^2-\bar{w}^2/4\right) \qquad (1)$$

where, $\bar{w}=\frac{r_o-r_i}{r_o}$ is the non-dimensional width of the slipper land.

The first group of the equation (1) corresponds the hydrostatic pressure distribution for flat and untilted slipper and the second group corresponds the hydrostatic pressure distribution produced by coning of the land and the tilt of the slipper. The final group represents the hydrodynamic effects due to conical shape of the land, slipper tilt and the slipper velocity.

The first group of the equation (1) can be replaced by an analytical solution of pressure for flat and untilt slipper which is derived in Appendix A. That analytical solution can be found out as $p=\frac{\ln(r/r_o)}{\ln(r_i/r_o)}\dot{p}_s$

Thus ultimately the equation of pressure distribution over the land of the slipper can be written as

$$\bar{p}=\bar{p}_s\frac{\ln\left(\bar{r}/\bar{r}_o\right)}{\ln\left(\bar{r}_i/\bar{r}_o\right)}+\frac{3\bar{p}_s}{2\bar{w}\bar{h}_c}\left(\bar{a}+\bar{t}\cos\theta_d\right)\left(\bar{z}^2-\frac{\bar{w}^2}{4}\right)+$$

$$\frac{3G}{\bar{h}_c^3}\left(\bar{a}\cos\theta+\bar{t}\cos\theta_m\right)\left(\bar{z}^2-\frac{\bar{w}^2}{4}\right).$$

Non-dimensional load is given as

$$\bar{W}=\int_0^{2\pi}\int_{-\bar{w}/2}^{+\bar{w}/2}\bar{p}\left(\bar{r}_c+\bar{z}\right)d\bar{z}\,d\theta$$

Putting the non-dimensional pressure the load carrying capacity can be derived as

$$\bar{W}=\frac{\pi\bar{p}_s\left(\bar{r}_o^2-\bar{r}_i^2\right)}{2\ln\left(\bar{r}_o/\bar{r}_i\right)}-\frac{2\pi\bar{p}_s\bar{r}_c\bar{w}^2}{4\bar{h}_o}\left[\frac{\bar{a}}{\sqrt{1-e^2}}+\frac{\bar{t}}{e}\left(1-\frac{1}{\sqrt{1-e^2}}\right)\right]$$

$$-\frac{G\bar{r}_c\bar{w}^3}{2\bar{h}_o^3}\cdot\frac{\pi\cos\theta_m}{\left(1-e^2\right)^{2.5}}\left[\bar{t}\left(2+e^2\right)-3e\bar{a}\right] \qquad (2)$$

Where

$\bar{h}_o=\frac{h_a-d}{h_a}$ and $e=\frac{\bar{t}\bar{r}_c}{1-\bar{d}}$

In equation (2) the first group is load carrying capacity for flat and untilted slipper. The second group is its modification for conical shape of the land and slipper tilt. The third group is the hydrodynamic effect on the load carrying capacity.

Finding out the appropriate G value is the main issue to solve the slipper equations. This is done from load equilibrium conditions. This analysis is different from Hook's analysis only by the equation of load equilibrium. The hydrodynamic parameter

$$G=\frac{\mu u r_o}{h_a^2 p_p}$$

which is dependent on h_a and

$$h_a = \left[6\mu r_o \sqrt{\frac{2}{\rho p_s}} \ln(r_o / r_i) \right]^{\frac{1}{2}}$$

The moment of the load with respect to x and y axis can be found out by integrating the load of small strip abut x and y axis. These moments are given by

$$\overline{M}_x = -\frac{\overline{p}_s}{4\overline{h}_o}\left(\overline{r}_c^{-2}\overline{w}^{-2} + \frac{\overline{w}^{-4}}{20}\right)\left[\frac{2\pi \sin\theta_m}{e}\left(1 - \frac{1}{\sqrt{1-e^2}}\right)\left(\overline{a} - \frac{\overline{t}}{e}\right)\right]$$

$$-\frac{G}{2\overline{h}_o^{-3}}\left(\overline{r}_c^{-2}\overline{w}^{-3} + \frac{\overline{w}^{-5}}{20}\right)\left[\frac{3\pi e \sin\theta_m \cos\theta_m}{\left(1-e^2\right)^{2.5}}\left(\overline{a}e - \overline{t}\right)\right]$$

and

$$\overline{M}_y = -\frac{\overline{p}_s}{4\overline{h}_o}\left(\overline{r}_c^{-2}\overline{w}^{-2} + \frac{\overline{w}^{-4}}{20}\right)\left[\frac{2\pi \cos\theta_m}{e}\left(1 - \frac{1}{\sqrt{1-e^2}}\right)\left(\overline{a} - \frac{\overline{t}}{e}\right)\right]$$

$$-\frac{G}{2\overline{h}_o^{-3}}\left(\overline{r}_c^{-2}\overline{w}^{-3} + \frac{\overline{w}^{-5}}{20}\right)\left[\frac{\pi \overline{a}\left(1+2e^2\right)\cos^2\theta_m}{\left(1-e^2\right)^{2.5}} + \frac{\pi \overline{a}\sin^2\theta_m}{\left(1-e^2\right)^{1.5}} - \frac{3\pi e\overline{t}\cos^2\theta_m}{\left(1-e^2\right)^{2.5}}\right]$$

From these two moments the load centre of the load can be found out by dividing the moment with the load carrying capacity. The derivations of the moments are given in Appendix C. Now the dimensional moments are given by

$M_x = \overline{M}_x.(r_o^3 p_p)$ and $M_y = \overline{M}_y.(r_o^3 p_p)$

The total moment on the land is given by

$$M = \sqrt{M_x^2 + M_y^2}$$

The polar arm of the load centre can be found out by

$$j = \frac{M}{W} = \frac{r_o\sqrt{\overline{M}_x^2 + \overline{M}_y^2}}{\overline{W}}$$

The angle between polar arm with the X axis is given by

$$\theta' = \tan^{-1}\frac{M_x}{M_y} - \frac{\pi}{2}$$

The abscissa and the ordinate of the load centre is given by

$j_x = j\cos\theta'$ and $j_y = j\sin\theta'$

III. Results

As the solution is directly got from the analytical method, the plotting can be done using MATLAB programming window. All the equation are set in the programming environment of the MATLAB software and the solutions are plotted. Generally the maximum clearance occurs very near to the leading edge. In the analysis of theoretical slipper drag, programming is developed with the fact that in the leading edge maximum clearance occurs. The position of the load centre is plotted against the slipper tilt. the slipper are considered as perfectly flat. For the figure 3, the slipper speed is kept constant at 1500 rpm and the plot is drawn for different pressure. It can be seen from the graph that after some point of tilt angle the position of load centre goes out of the slipper land area. This prove that slipper runs with very small tilt angle. For figure 4 the pressure is kept constant at 120 bar and the plot is drawn for different speeds. It is observed for a higher theoretical tilt the slipper does not work. Apparently the fluid film breaks after a maximum angle of tilt.

It can be observed from figure 3 through figure 6, that the slipper center stays in the center line of motion or X axis for small tilt angles. For small tilt angle the center of load moves firstly towards the negative X axis. More tilt brings the center of load on the positive side of X axis. A little more tilt bring the centre of load to the actual centre of slipper. But for more tilt angle the centre of tilt angle the load goes outside the area of slipper which is not possible. Therefore a higher tilt is not possible to occur in actual slipper operation. Moreover the variation of pressure, speed, slipper area and non flatness angle put different response to the position of load centre. It can be observed that higher pressure in the slipper pocket tries to keep the slipper load centre in the actual centre of slipper and lower pressure tries to deflect the load centre away from actual slipper centre. In the same way higher speed of slipper tries to keep the slipper load centre in the actual centre of slipper and lower speed tries to deflect the load centre away from actual slipper centre. From figure 5, it can be observed that a particular amount of non-flatness angle tries to keep the load centre in the actual slipper centre.

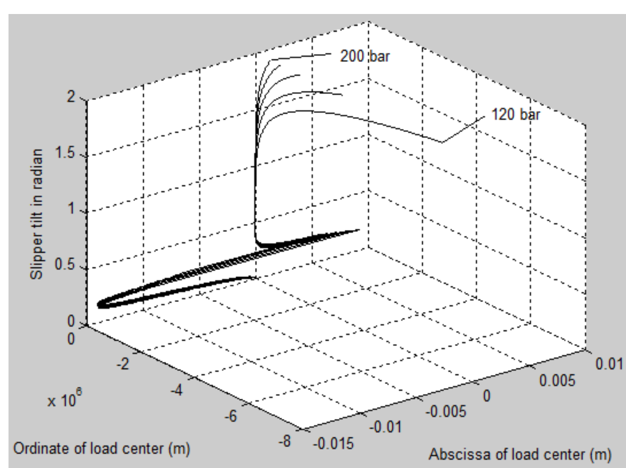

Figure 3 : Position of load centre with slipper tilt for different pressure

From figure 6, it can be observed that a more amount of slipper are tries to keep the load centre in the actual slipper centre and hence stabilize the bearing fast.

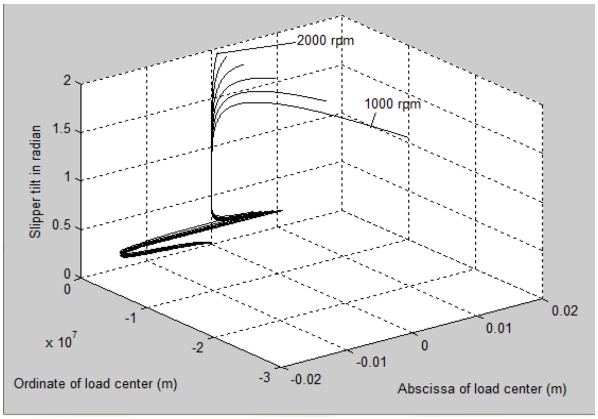

Figure 4 : Position of load centre with slipper tilt for different slipper area

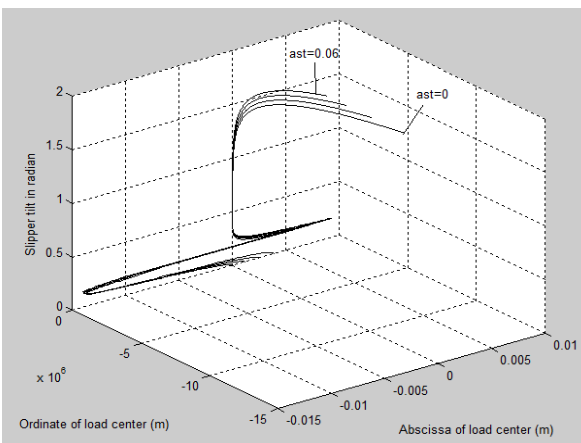

Figure 5 : Position of load centre with slipper tilt for different non flatness angle

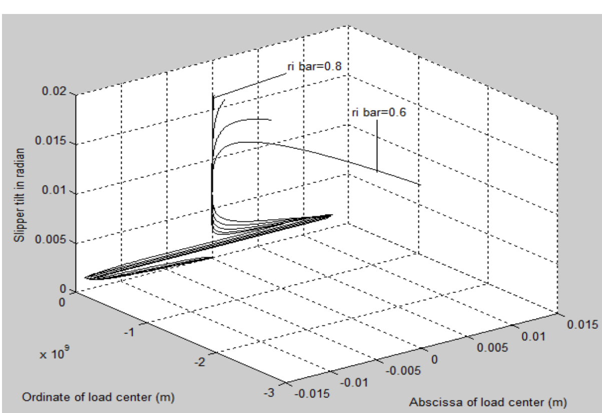

Figure 6 : Position of load centre with slipper tilt for different slipper area

IV. Conclusion

From the results of the computation of the position of load centre, it can observed that higher tilt angle gives irrelevant results. It may happen the fluid film breaks at higher tilt angles. The stability of slipper increases with increase of slipper pressure (vide figure 3). The stability increases with increase of slipper speed (vide figure 4). The stability of slipper increases with increase of slipper non flatness angle (vide figure 5). The stability increases with increase of slipper land size (vide figure 6). For more practicality of this tilt angle more computation is required.

References Références Referencias

1. E. Koc and C. J. Hooke, “Investigation into the effects of orifice size offset and over clamp ratio on the lubrication of slipper bearings,” *Tribology International*, vol. 29, no.4, pp. 299-305, 1996.
2. X. Wang and A. Yamaguchi, “Characteristics of hydrostatic bearing/seal parts for water hydraulic pumps and motors. Part 1: Experiment and theory,” *Tribology International*, vol. 35, pp. 425–433, 2002.
3. X. Wang and A. Yamaguchi, “Characteristics of hydrostatic bearing/seal parts for water hydraulic pumps and motors. Part 2: On eccentric loading and power losses,” *Tribology International,* vol. 35, pp. 435–442, 2002.
4. N. D. Manring, R. E. Johnson, and H. P. Cherukuri, “The impact of linear deformations on stationary hydrostatic thrust bearings,” *American Society Mechanical Engineers, Journal of Tribology,* vol. 124, pp. 874–877, 2002.
5. N. D. Manring, “Experimental Studies on the Performance of Slipper Bearings within Axial-Piston Pumps,” *American Society Mechanical Engineers, Journal of Tribology*, vol. 126, pp. 511–518, 2004.
6. S. L. Nie, “Tribological study on hydrostatic slipper bearing with annular orifice damper for water hydraulic axial piston motor,” *Tribology International*, vol. 39, pp. 1342–1354, 2006.
7. S. Kumar, J.M. Bergada, and J. Watton “Axial piston pump grooved slipper analysis by CFD simulation of three-dimensional NVS equation in cylindrical coordinates.” *Computers & Fluids* Vol. 38 pp-648–663, 2009
8. M. Borghi, E. Specchia, and B. Zardin, “Numerical Analysis of the Dynamic Behaviour of Axial Piston Pumps and Motors Slipper Bearings,” *SAE International Journal of Passenger Cars- Mechanical Systems*, vol. 2, no. 1, pp-1285-1303, 2009.
9. H. Liu, Z. Xiong, and C. J. Shen, “Film Shape Research of Slipper Bearing in Axial Piston Pump Based on Genetic Algorithms,” *Advanced Materials Research*, vol. 301 – 303, pp-1533-1538, 2011.

Global Journal of Researches in Engineering (A) Volume XII Issue V Version I Year 2012

10. F. Canbulut, E. Koç, and C. Sinanoglu, "Design of artificial neural networks for slipper analysis of axial piston pumps," *Industrial Lubrication and Tribology*, vol. 61, no. 2, pp.67 – 77, 2009.
11. E. Koc, "Slipper balance in axial piston pumps and motors," *American Society Mechanical Engineers, Journal of Tribology*, vol. 114, pp. 766-772, 1992.
12. C. J. Hooke and Y. P. Kakoullis, "The Effect of Non-Flatness on the Performance of Slippers in Axial Piston Pumps," *Proceedings of Institutions of Mechanical Engineers,* vol. 197C, pp. 239-247, 1983. E. Koc and C. J. Hooke, "Consideration in the design of partially hydrostatic slipper bearings," *Tribology International*, vol. 30, no. 11, pp. 815-823, 1997.
13. C. J. Hooke and Y. Li K, "The Lubrication of Over clamped Slipper in Axial Piston Pumps," *Proceedings of Institutions of Mechanical Engineers,* vol. 202, no. C4, pp. 117-123, 1988.
14. C. J. Hooke and Y. Li K, "The lubrication of slippers in axial piston pumps and motors," *Proceedings of Institutions of Mechanical Engineers*, vol. 203, pp. 343-350, 1989.
15. N. Iboshi and A. Yamaguchi ," Characteristics of a slipper bearing for swash plate type axial piston pump and motor," *Bulletin of Japan Society Mechanical Engineers*, vol. 26, no. 219, pp. 1583-1589 ,1983.
16. E. Koc, "Slipper balance in axial piston pumps and motors," *American Society Mechanical Engineers, Journal of Tribology*, vol. 114, pp. 766-772, 1992.
17. F. Canbulut, "Design of an artificial neural network for analysis of frictional power loss of hydrostatic slipper bearings," *Journal of Tribology*, vol. 17, no. 4, pp. 887 – 899, 2004.
18. A. Crook and M. J. Fisher, "An investigation into the dynamic behavior of hydrostatic slipper bearing," *BHRA Report* RR 1023, 1969.
19. S. V. Cunningham and D. McGillivray, "The design and operation of hydrostatic slipper pad bearings in hydrostatic motors," *Proceedings of Institutions of Mechanical Engineers*, vol. 180, no. 3L, 1966.
20. M. J. Fisher, "A theoretical determination of some characteristics of tilted hydrostatic slipper pad," *BHRA Report* RR728, 1962.
21. R. M. Harris, "Slipper pads in swash-plate type axial piston pumps," *Journal of Dynamic Systems Measurements and Control*, vol. 118, pp. 41-47, 1996.
22. W. D. Milestone, "The Kinematic Analysis of Axial-Piston Pumps," *Mechanism and Machine Theory*, vol. 18, no. 16, pp. 475-479, 1983.
23. N. D. Manring, "The Torque on the Input Shaft of an Axial Piston Swash Plate Type Hydrostatic Pump," *Journal of Dynamic Systems Measurements and Control*, vol. 120, no. 1, pp. 57-62. 1998.
24. N. A. Shute, I D. E. Turnbul, "The minimum power loss of hydrostatic slipper bearing*," BHRA Report* SP721, 1962(a).
25. N. A. Shute, I D. E. Turnbul, "The losses of hydrostatic slipper bearing under various operating conditions," *BHRA Report* SP743, 1962(b).